

In the next section the general characteristics of the winds and waves affecting the East Coast of Korea are described along with a description of the available data. In Section 3 the wave model is described and in Section 4 the applied data assimilation technique and its settings are described. A 32 days long period - from 17 November 2015 until 16 December 2015 - has been considered in the evaluation of the model hindcast and analysis. This period has been judged to provide a variety of storm conditions allowing a proper assessment of the wave modelling and data assimilation, which is given in Section 5. The article ends with final remarks in Section 6.

2 Data and system understanding

2.1 General characteristics

The surface winds over the East Sea of Korea are generally mild or moderate and variable in summer and can be very strong in the winter, caused by low pressure systems in the East Asia winter monsoon. Typhoons occur from July through October, reaching their peak frequency in September. However, they generally move northwards in the East Sea of Korea, leading to no extreme wave conditions along the east coast of Korea. Due to the regional monsoon variations, winds are predominately from the northwest to northeast in the winter and more predominant from the northeast in the summer. Due to extra-tropical storms, there is a strong and predominant western-north-western wind from November to February. Along the Northeastern coast of Korea the most frequent, extreme and longer waves come for the Northeast.

In order to describe the mean wave climate in the region in more detail wind and wave reanalysis data from the European ReAnalysis interim (ERA-interim, Dee et al., 2011) dataset of the European Centre for Medium-range Weather Forecasts (ECMWF) has been used. The strength of the ERA-interim dataset is that it combines one of the leading numerical weather prediction models (the ECMWF model) with an advanced data assimilation system (Dee et al., 2011). The ERA-interim wave data are, therefore, known for its high quality, which is reflected in the high correlation between ERA-interim wave data and observations. However, due to its coarse resolution of about 80km x 80km resolution the dataset is known to underestimate extreme wave events and of not being capable of fully solving tropical cyclones. Although, thanks to the used data assimilation scheme, even for small systems some tropical cyclone information is present in the ERA-interim data, the data are not suitable for analyses of tropical cyclones. The ERA-interim data from 1979 to 2016 is used next to provide a description of the wind and wave climate in the region, keeping the mentioned caveats due to resolution in mind.

Figure 2 shows the monthly roses of the 10 m height wind speed (U_{10}) and direction (U_{dir}) and Figure 3 shows the monthly roses significant wave height (H_s) and mean wave period¹ ($T_{m-1,0}$) and mean wave direction (MWD) for a location offshore the Northeast coast of Korea (130.5°E, 37.5°N). As can be seen in the figure, in the region winds blow from almost all directions although being less frequent from the North and from the South and the most frequent, extreme and longer waves come for the Northeast. There are also extreme waves from the West-Northeast in line with the wind climate. Figure 2 shows also the expected monsoon variations, with wind predominantly from the western to north-eastern sectors (from the Asian continent) and more predominately from the northwest in the winter and from the north-eastern to south-western sectors (from the Northern Pacific) and more predominately from the northeast in the summer. Due to extra-tropical storms, there is a strong and predominant western-north-western wind from November to February. The wave roses show that during the whole year the most extreme and longer waves come from the Northern half, West to Northeast, cf. Figure 3.

¹ There are several parameters for describing the sea state period. One of these is $T_{m-1,0} = m_{-1}/m_0$ where m_n , the n order spectral moment, is $m_n = \int_0^\infty f^n S(f) df$, f is the frequency and $S(f)$ the spectral wave energy. Using different moments other period parameters can be defined. Such as $T_{m0,1} = m_0/m_1$ and $T_{m0,2} = \sqrt{m_0/m_2}$. Another commonly used wave period is the peak wave period, T_p , the period corresponding to the spectral maximum.

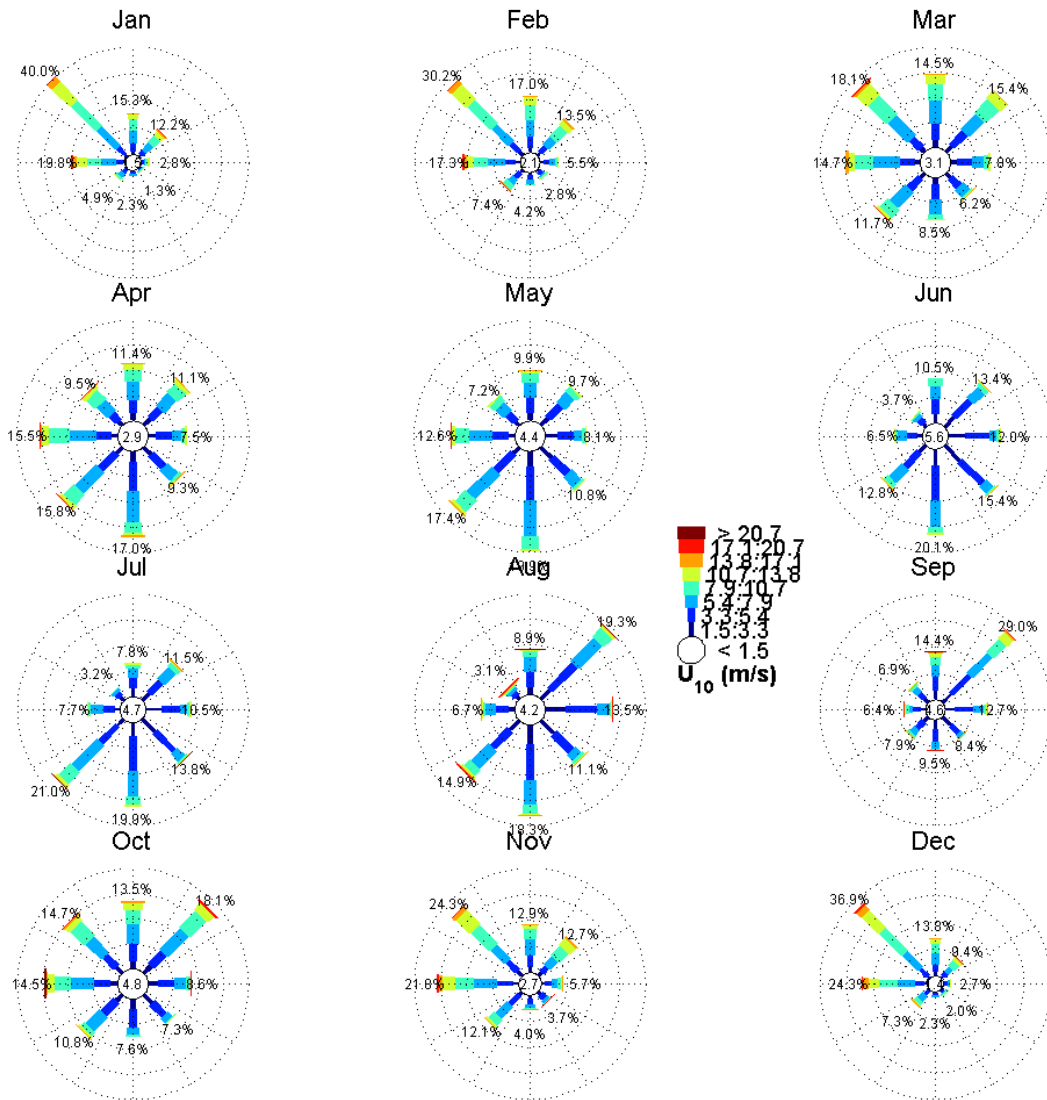


Figure 2 Monthly roses of ERA-interim wind speed data from 1979 to 2016 at 130.5°E and 37.5°N. The values plotted inside the circle on the centre of each rose represent the percentage of values that are below the lowest considered class of the variable being presented (e.g., below 1.5 m/s), the arrow length of each of the colours in the roses is the percentage of occurrence of conditions within a certain bin, the direction shown by each arrow/ray represents the direction from which winds (or waves) are coming from.

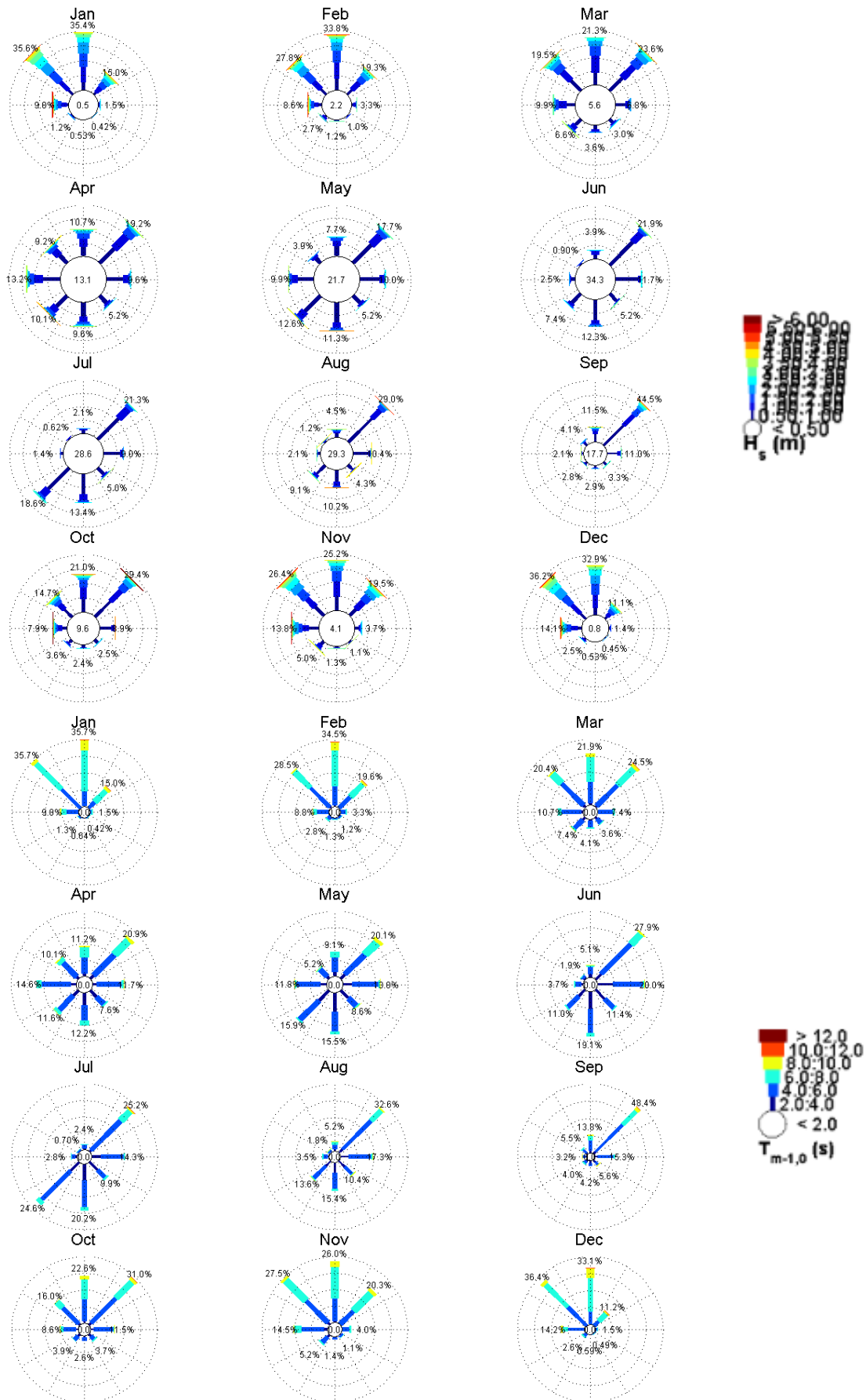


Figure 3 Monthly roses of ERA-interim significant wave height (top) and mean wave period (bottom) data from 1979 to 2016 at 130.5°E and 37.5°N.

2.2 Observations

Along the Eastern coast of Korea wave and wind observations are available at the locations shown in Figure 1. The coordinates of these locations, local depths and variables being observed are given in Table 1. Further details, such as the operator and the type of instrument, are as follows:

- MB – KIOST directional wave spectra observations from an AWAC (<http://www.nortek-as.com/en/products/wave-systems/awac>) directional wave gauge.
- WJ – KIOST directional wave spectra observations from an AWAC directional wave gauge.
- DH – Korean Meteorological Administration (KMA) significant wave height, peak wave period and mean wave direction observations from a large directional wave buoy anchored to the bottom. Wind speed and direction measured at 10 m height from an anemometer at an Automatic Weather Station (AWS) mounted on the buoy.
- UL – KMA significant wave height, peak wave period and mean wave direction observations from a large directional wave buoy anchored to the bottom. Wind speed and direction measured at 10 m height from an anemometer at an AWS mounted on the buoy.
- E01 – Korean Hydrographic and Oceanographic Agency (KHOA) significant wave height, peak wave period and mean wave direction observations from a Korea Ocean Gate Array (KOGA) buoy having a directional wave sensor. Wind speed and direction measured at 10 m height from an anemometer at an AWS mounted on the buoy.
- E02 – KHOA directional integral wave parameter observations from a KOGA buoy having a directional wave sensor. Wind speed and direction measured at 10 m height from an anemometer at an AWS mounted on the buoy.

Location	Longitude (°)	Latitude (°)	Depth	Variables
MB	129.219	37.410	18.7 m	Directional wave spectra
WJ	129.416	37.079	25.9 m	Directional wave spectra
DH	130.000	37.533	Deep ($\approx 1,500$ m)	$H_s, T_p, MWD, U_{10}, U_{dir}$
UL	131.100	37.450	Deep ($\approx 2,100$ m)	$H_s, T_p, MWD, U_{10}, U_{dir}$
E01	131.540	38.001	Deep (≈ 900 m)	$H_s, T_p, MWD, U_{10}, U_{dir}$
E02	130.564	37.722	Deep ($\approx 1,200$ m)	$H_s, T_p, MWD, U_{10}, U_{dir}$

Table 1 Coordinates of the observation locations and local depths.

2.3 Operational models

There is a number of local wave models from which data are available for this region, namely:

- KOOS-WAM: A coarse (20 km x 20 km) WAM model covering the region shown in Figure 4 and operated by the project Korea Operational Oceanographic System (KOOS) of KIOST.
- KOOS-WW3: A coarse (20 km x 20 km) WW3 model covering the same region as the KOOS-WAM model and with a finer resolution (4 km x 4 km) WW3 model covering the South Korean waters nested on it, see Figure 4. These nested WW3 models are also operated by the project KOOS of KIOST.
- KMA-CWW3: A coastal (1 km x 1 km) WW3 model (CWW3), which is nested in a regional (8 km x 8 km) WW3 model and which in turn is nested in a global (50 km x 50 km) WW3 model. The domains of the models, which are operated by the Korean Meteorological Administration (KMA, http://web.kma.go.kr/eng/biz/forecast_02.jsp) are outlined in Figure 4.

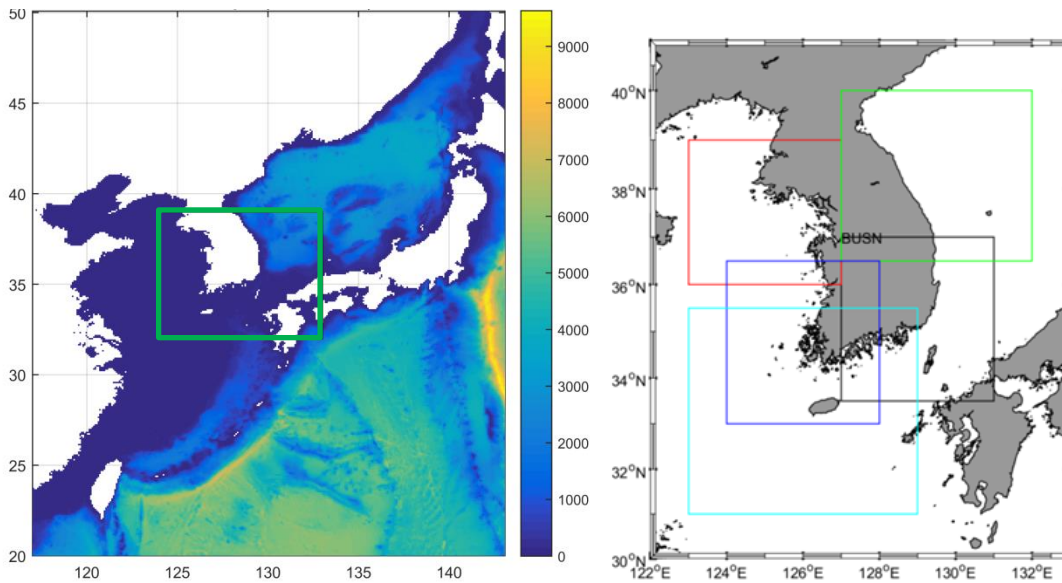


Figure 4 Left panel: Region covered by the coarse KOOS-WAM and KOOS-WW3 models, with the region covered by the nester finer resolution WW3 model outlined in green. The scale of the shown bathymetry is given in metres in the right. Right panel: Region covered by the coastal WW3 (CWW3) models operated by KMA. Results from the model with the domain outlined in green have been made available for this project.

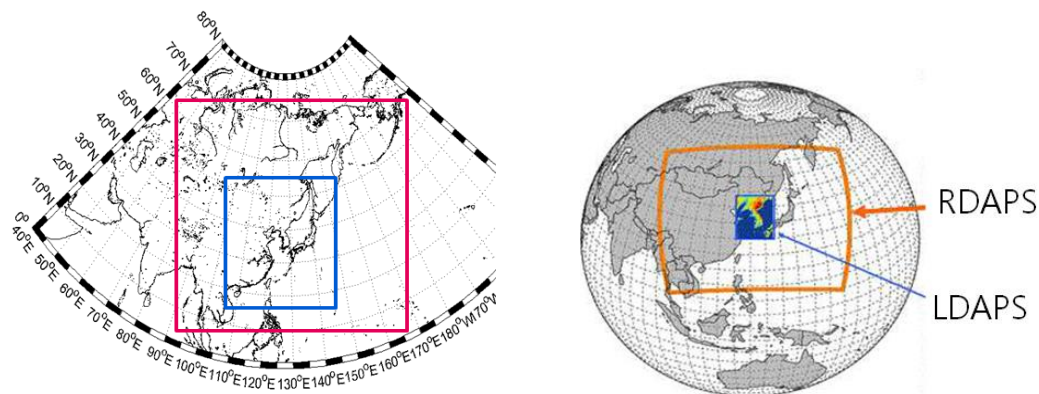


Figure 5 Left panel: Outline of the domains of the KIOST-WRF atmospheric model, for both domains the model resolution is 20 km x 20 km. Right panel: Outline of the domains of the KMA-UM atmospheric models, in the RDAPS domain the model resolution is 12 km x 12 km and in the LDAPS domain 1.5 km x 1.5 km.

There is also a number of local numeric weather prediction (NWP) models from which data are available for this region, namely:

- KIOST-WRF: KIOST operates a Weather Research and Forecasting (WRF, <http://www.wrf-model.org>) model with 3D-VAR data (synop, sounding, buoy, scatterometer) assimilation (Heo and Ha, 2016). The model domains are outlined in Figure 5. There is a wide domain with a 20 km x 20 km resolution with a smaller domain with a resolution of also 20 km x 20 km nested on it (there is still smaller domain with a finer resolution of 4 km x 4 km, but it does not cover the whole East Sea of Korea). The model gets initial conditions from the Global Forecast System (GFS) of the American National Centers for Environmental Prediction (NCEP). Hourly 10-m wind fields are available from the WRF model.
- KMA-UM: KMA operates a regional Unified Model (UM, https://en.wikipedia.org/wiki/Unified_Model) with four-dimensional variational data assimilation (4D-VAR), see http://web.kma.go.kr/eng/biz/forecast_02.jsp. Three-hourly 10 m wind fields with a spatial resolution of 12 km x 12 km are available from a regional UM model (referred to as Regional Data Assimilation and Prediction System, RDAPS). There is also a local UM model (referred to as Local Data Assimilation and Prediction System, LDAPS) with a spatial resolution of 1.5 km x 1.5 km and not covering the wave model

domain and from which winds were not available for the considered period. The domain covered by these models and given in Figure 5.

3 Wave model

3.1 Introduction

In order to obtain the best compromise between computational accuracy and efficiency, two nested models, namely the

- Overall Model – a coarse resolution model covering the East Sea of Korea and the
- Coastal Model – a finer resolution model covering the Northeastern coastal strip of South Korea, extending from the coast into deep waters

were employed. Accordingly, the wave modelling is carried out in two stages with corresponding model domains which are outlined in Figure 6. In these domains computational rectangular grids were defined in spherical coordinates (longitude, latitude) using the WGS84 geodetic datum.

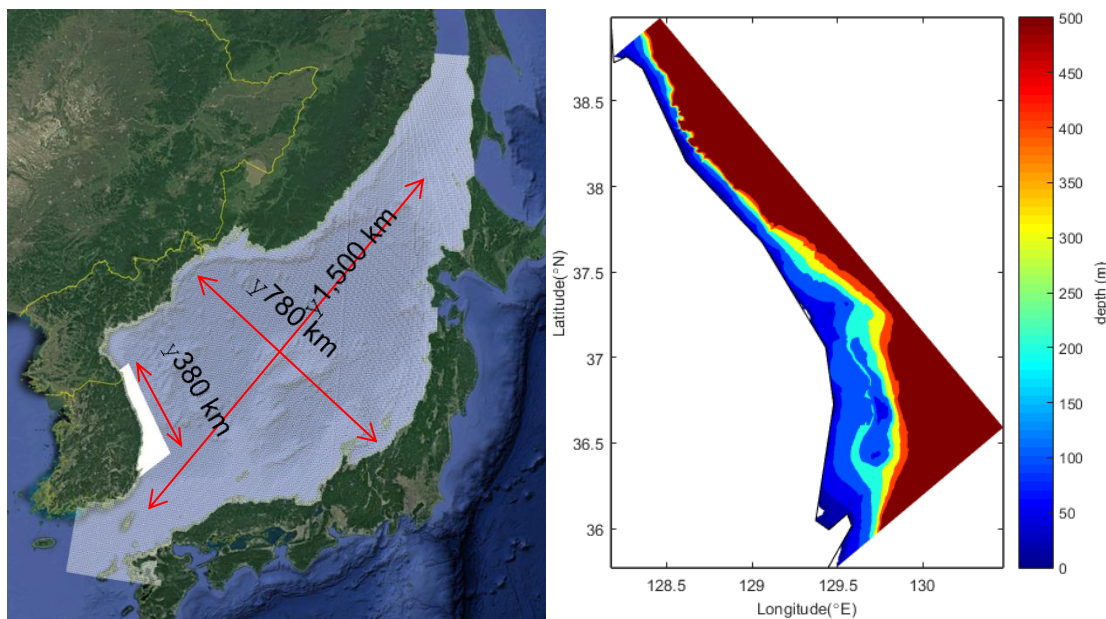


Figure 6 Right panel: Coverage and approximate dimensions of the Overall (light blue) and Coastal (white) Model grids. Left panel: Bathymetry of the Coastal Model.

3.2 Overall Model

A number of factors were taken into consideration in the definition of the Overall Model grid and domain. Recognising the primary importance of the waves generated in the East Sea of Korea to the Northeastern coast of Korea (cf. §2.1) the model was set to cover the whole East Sea of Korea. In order to also account for the relatively frequent waves entering the East Sea of Korea from the South, the model covers the Strait of Korea and extends into the East China Sea, where wave boundary conditions are imposed. The resolution of the Overall Model is of about 5 km x 5 km (about 45,000 active grid points). The model bathymetry, which is shown in Figure 1, was derived from the American etopo5 database (<http://www.ngdc.noaa.gov/mgg/global/etopo5.HTML>) and the bathymetry of the Coastal Model in the region covered by it.

3.3 Coastal Model

The purpose of the Coastal Model was to allow the modelling of depth effects with more resolution and therefore accuracy. The resolution of the Coastal Model is of about 300 m x 300 m (about 250,000 active grid points). The model extends from the coast into deep waters, covering the nearshore MB and WJ observation locations. The model bathymetry, which is show in Figure 6, was derived using the KorBathy30s bathymetry database (Seo, 2008) and detailed survey data from KHOA with a resolution of about 150 x 150 m. Sensitivity tests have been carried out

considering a grid with a resolution of about 150 m x 150 m, but the extra computational effort did not pay off in terms of accuracy of the results at the coastal buoy locations.

3.4 Directional and spectral grids

Each SWAN wave model requires the specification of three grid types:

1. a computational grid which defines the geographical location in 2D-space of the grid points and which have been described above;
2. a directional grid which defines the directional range (usually 360°) and resolution;
3. a spectral grid which defines the range and resolution of the grid in frequency space.

In both the Overall and Coastal models the same directional and spectral grids were defined. For directional space, the full circle is considered, divided in 48 sectors of 7.5° each. For the frequency domain frequencies were set to range from 0.03 to 1.5 Hz (0.67 s – 33.33 s) logarithmically divided in 41 bins.

3.5 Boundary waves

When the models will be operational the wave parameters from the KOOS-WAM model will be available as boundary waves for the Overall Model. Figure 7 shows the locations of the KOOS-WAM data that are to be imposed in the southern boundaries of the Overall Model. These wave conditions are given parametrically in terms of significant wave height, peak wave period and mean wave direction. For each set of conditions a JONSWAP spectra is assumed in SWAN with a peak enhancement parameter of 3.3 and a directional spreading of about 31°. The conditions are set to vary linearly between two input locations along the model boundary. The conditions are kept constant between the coast line and the closest input location along the model boundary.

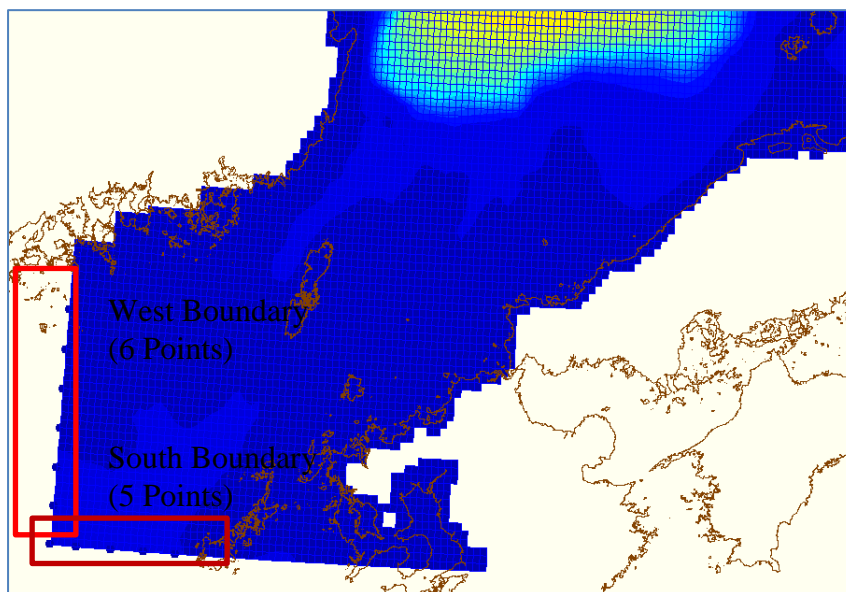


Figure 7 Boundary locations of the Overall Model where boundary wave conditions are prescribed.

3.6 Wind fields

When the models will be operational the KIOST-WRF winds will be available and used to force the Coastal and Overall models. It is, therefore, of importance to validate the models forced with the WRF winds. However, given that the coastal and overall model results will also be compared with KMA-WW3 model results it is also of interest to validate the results of the models forced with the KMA's UM wind fields. Time and space varying wind fields from the KIOST-WRF model, with a spatial resolution of 20 km x 20km and a temporal resolution of 1 hour, are used to force the wave models. Furthermore, RDAPS time and space varying wind fields from the KMA-UM model, with a spatial resolution of 12 km x 12 km and a temporal resolution of 6 hour, are used to force the wave models. The wind fields resulting from the data assimilation, which have a spatial and temporal resolution equal to that of the first guess KIOST-WRF winds, will also be used to force the Overall and Coastal models.

3.7 Overall model settings

The SWAN wave modelling is carried out in non-stationary, 3rd generation mode for wind input, quadruplet interactions and whitecapping (wave steepness induced wave breaking). The default options of the applied SWAN version 40.85 are applied to all numerical and physics settings except for:

- Wind growth and whitecapping: Komen et al. (1984) with the settings recommended by Rogers et al. (2003) for wind growth and whitecapping is applied.
- Bottom friction: The JONSWAP formulation (Hasselmann et al., 1973) is applied with a friction coefficient of $0.038\text{m}^2\text{s}^{-3}$ as recommended by Zijlema et al. (2012).
- Numeric scheme: A first-order backward space, backward time (BSBT) scheme is applied.
- Integration time step: A fixed time step of 20 min is applied.
- Accuracy: The solver is set to stop when the changes in the solution are of less than 1% in H_s and $T_{m0,1}$ at 99% of the grid points relatively to the previous iterations, with a maximum of 99 iterations per timestamp.

Furthermore a uniform water level of 0 m MSL is considered in all computations.

4 Data assimilation

4.1 Methodology

The data assimilation will be carried out by means of Ensemble Kalman Filter (EnKF) using the Open Data Assimilation (OpenDA) toolbox (<http://www.opendata.org>) to which the SWAN model is connected through a black-box wrapper.

In an EnKF the model uncertainty is computed from an ensemble of model predictions in a procedure very similar to Monte Carlo methods (Evensen, 2003). The analysis or measurement-step of the EnKF uses a perturbation of the observations and a separate analysis for each of the ensemble members to obtain a consistent ensemble of model states that incorporate the observations. If required one can obtain the mean and covariance of the model state after the analysis. More precisely, starting from an initial ensemble of model states $\xi_i^a(t_0)$ the model M is used to compute a forecast for each ensemble member:

$$\xi_i^f(t_{k+1}) = M \xi_i^a(t_k) + w_i(t_k),$$

where $w_i(t_k)$ denote the system noise, used to model uncertainties in the model. From this one can compute the sample mean as

$$x^f(t_k) = 1/n \sum_{i=1}^n \xi_i^f(t_k)$$

and covariance

$$\mathbf{P}^f(t_k) = 1/(n-1) \sum_{i=1}^n (\xi_i^f(t_k) - x^f(t_k))(\xi_i^f(t_k) - x^f(t_k))'$$

The Kalman gain is expressed as

$$\mathbf{K}(t_k) = \mathbf{P}^f(t_k) \mathbf{H}' (\mathbf{H} \mathbf{P}^f(t_k) \mathbf{H}' + \mathbf{R})^{-1},$$

where \mathbf{H} denotes the observation operator that maps the model state to values that match the observations. \mathbf{R} is the error covariance of the observations at time t_k .

The analysis or measurement-step of the EnKF uses a perturbation of the observations $v_i(t_k)$ and a separate analysis for each of the ensemble members to obtain a consistent ensemble of states that incorporate the observations $y(t_k)$,

$$\xi_i^a(t_k) = \xi_i^f(t_k) + \mathbf{K}(t_k)(y(t_k) - \mathbf{H} \xi_i^f(t_k) - v_i(t_k))$$

If required one can obtain the mean and covariance of the model state after the analysis, that can be computed from

$$x^a(t_k) = 1/n \sum_{i=1}^n \xi_i^a(t_k),$$

and

$$\mathbf{P}^a(t_k) = 1/(n-1) \sum_{i=1}^n (\xi_i^a(t_k) - x^a(t_k))(\xi_i^a(t_k) - x^a(t_k))'.$$

The OpenDA implementation for SWAN uses the full wave spectra at all grid-cells as the state of the model. Two likely sources of uncertainty in a spectral wave model are the uncertainty in the wind forcing and uncertainty for the wave parameters that are specified at the open-boundary. These are also the sources that can be considered in the OpenDA implementation of EnKF for SWAN (see e.g. Serpoushan et al., 2013).

4.2 Settings

The results of the EnKF data assimilation in SWAN are sensitive to a number of parameters, such as 1) uncertainty in the specification of the forcing winds and boundary waves (the so-called control variables), 2) which data are assimilated and their uncertainty and 3) the number of EnKF ensemble members:

- 1) In this study we only considered uncertainty for the wind forcing. The uncertainty in the boundary waves is not considered to be as crucial for the quality of the results and is, therefore, not considered in these experiments. The used (first-guess) wind fields are the WRF fields. For the uncertainty in the wind forcing, the two wind components are treated independently. For each component the errors are assumed to be spatially and temporally correlated with an exponential decay with distance and time-difference. The error standard deviation is set to 1 m/s, the temporal and spatial correlation reach the value 0 after 12 hours and at 500 km distance, respectively.
- 2) Observations of H_s have been assimilated every hour at the further offshore DH and E01 locations (cf. Figure 1). The standard deviation for errors in the observations was set to 0.2m and uncorrelated Gaussian white-noise has been applied.
- 3) Experimental runs were carried out with 10, 30 and 100 ensemble members. The number of ensemble members did not affect the results much but the observation minus model statistics of the run with 30 ensembles were slightly better.

To reduce the EnKF computational effort the Overall Model computational grid has been coarsened nine times from a resolution of $0.05^\circ \times 0.05^\circ$ to a resolution of $0.45^\circ \times 0.45^\circ$, see Figure 8. Furthermore, although SWAN can read wind fields in curvilinear grids that is not the case for OpenDA, which only supports rectangular grids for the wind. The WRF input winds had therefore to be mapped into a rectangular grid for the EnKF experiments. The used rectangular grid had a resolution close to that of the original WRF fields, see Figure 8. The resulting analysis wind fields have then been used to force the full (not coarsened) Overall Model and nested Coastal Model.

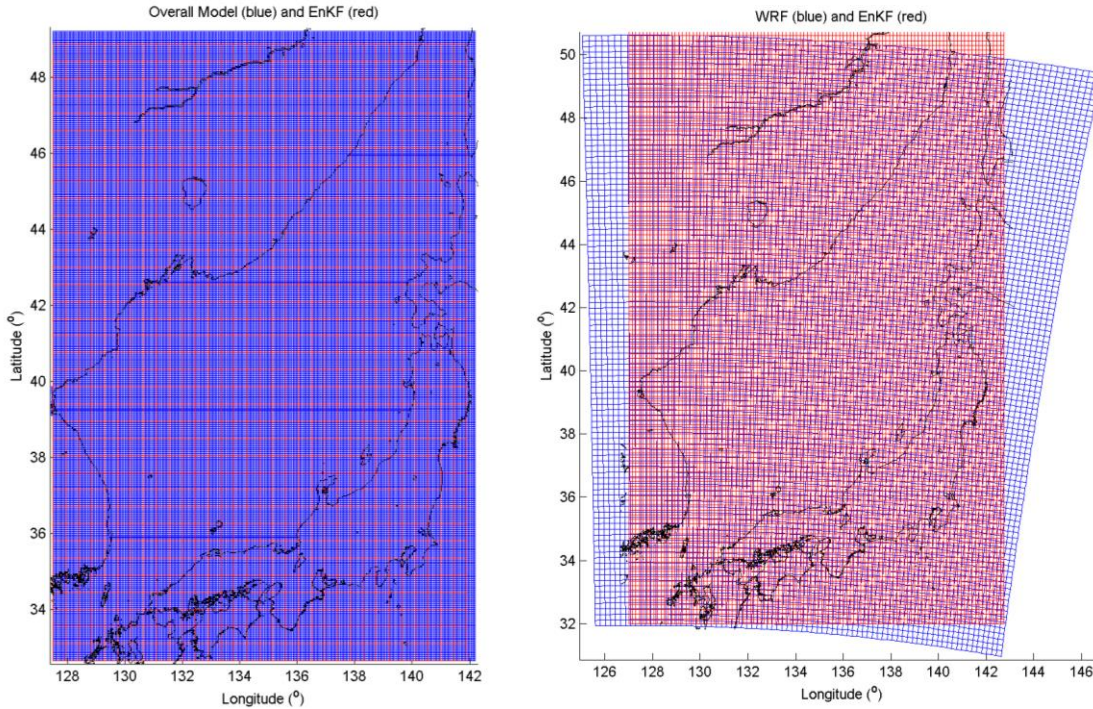


Figure 8 Left Panel: Grid of the Overall Model (blue) and grid of the model used in the EnKF runs (red). Right panel: Grid of the KIOST-WRF winds used in the hindcast (blue) and grid of the winds used in the EnKF runs (red).

5 Analysis of the results

Figures 9 to 14 show the comparisons between the H_s , T_p and MWD observations and the model results at MB, WJ, DH, UL, E01 and E02. In total six wave model results are considered:

- SWAN: The (default) SWAN hindcast with the KIOST-WRF wind forcing;
- SWAN-UM: The SWAN hindcast with the KMA-UM wind forcing;
- SWAN-EnKF: The SWAN hindcast with the analysed wind forcing, by means of EnKF data assimilation of the KIOST-WRF winds, we refer to these winds as EnKF winds and refer to these SWAN results also as analysis (i.e. 0h hindcasts/forecasts with data assimilation);
- KMA-CWW3; KOOS-WW3 and KOOS-WAM (cf. §2.3).

Figures 15 to 18 show the comparisons between the U_{10} , U_{dir} observations and the KIOST-WRF, KMA-UM and EnKF results at DH, UL, E01 and E02.

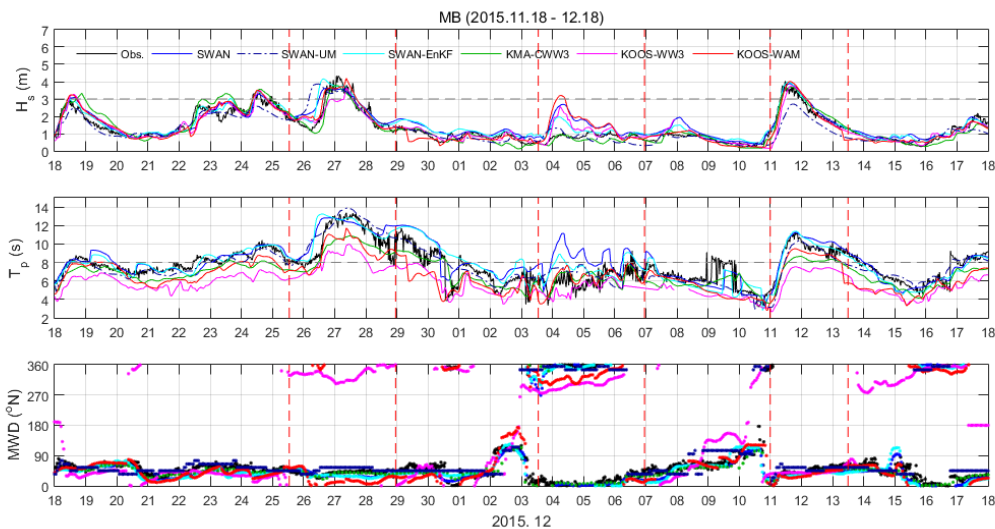


Figure 9 Time series of the MB wave observations and wave model results.

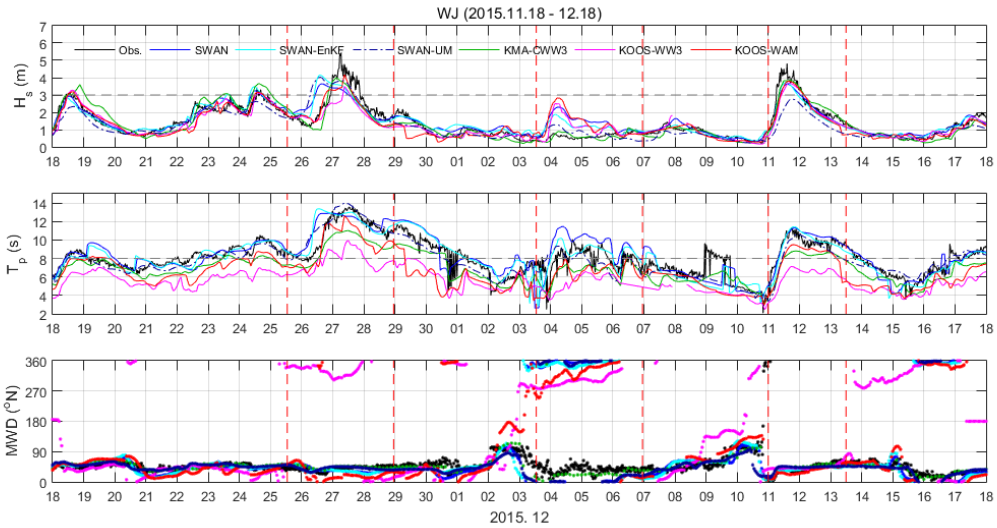


Figure 10 Time series of the WJ wave observations and wave model results.

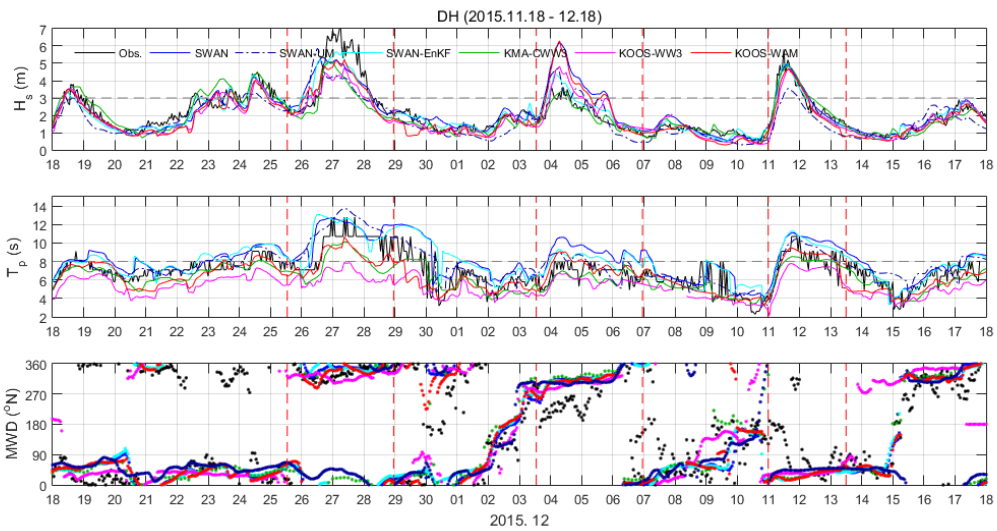


Figure 11 Time series of the DH wave observations and wave model results .

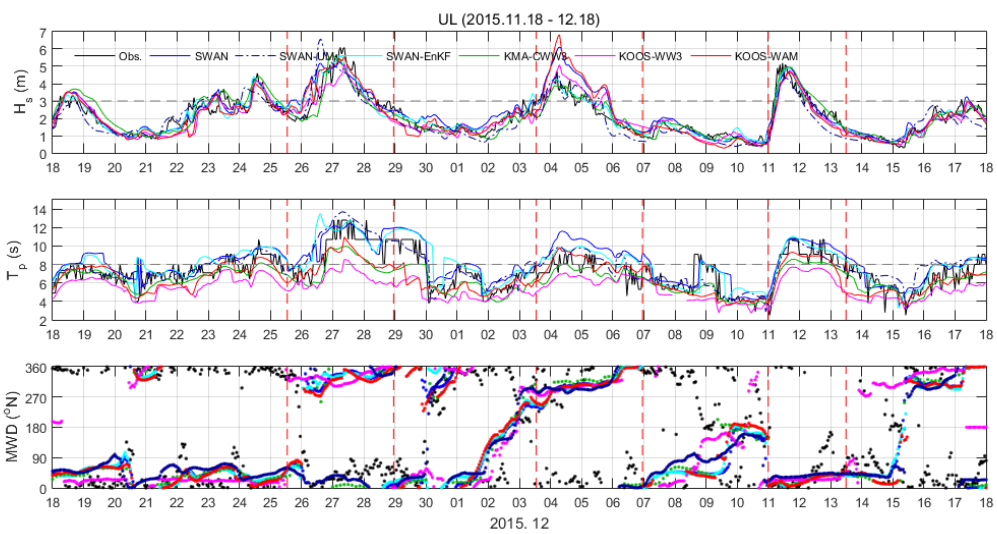


Figure 12 Time series of the UL wave observations and wave model results.

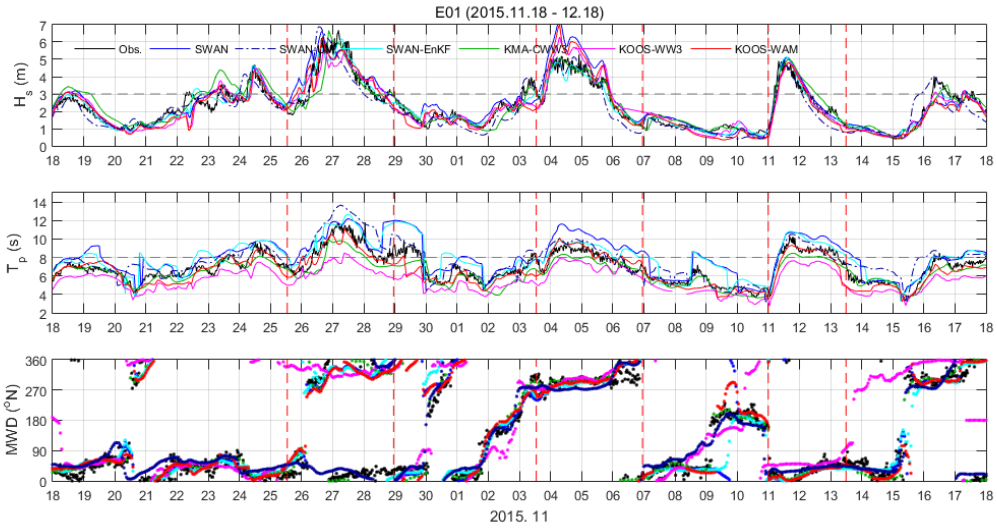


Figure 13 Time series of the E01 wave observations and wave model results.

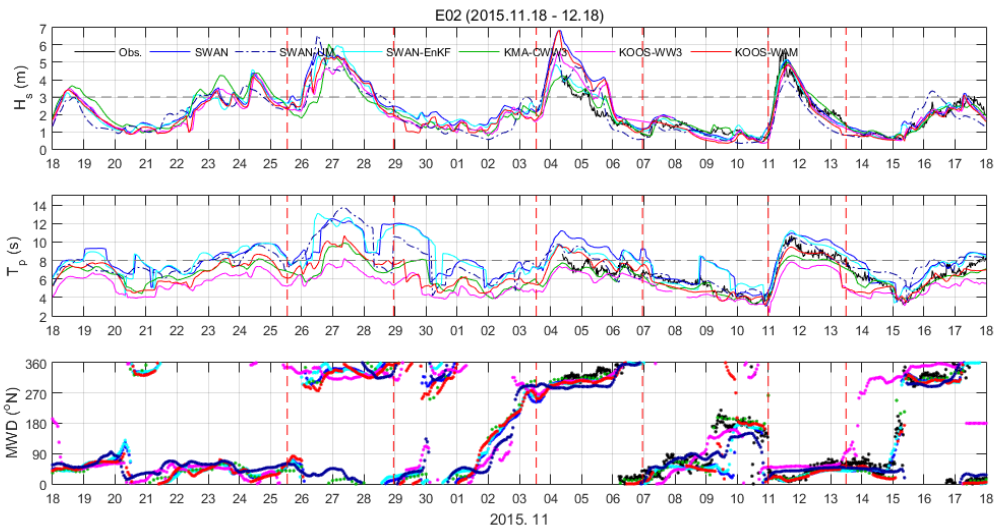


Figure 14 Time series of the E02 wave observations and wave model results.

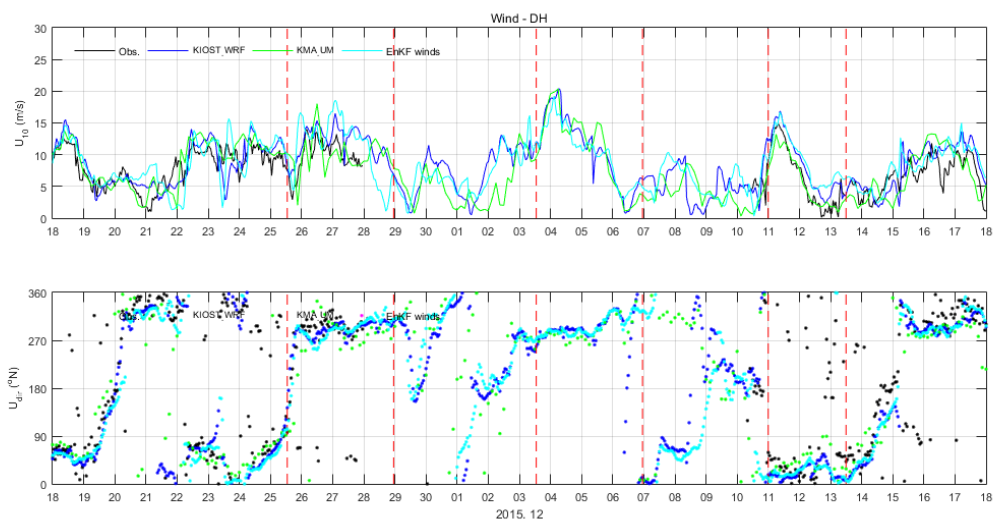


Figure 15 Time series of the DH wind observations and KIOST-WRF, KMA-UM and EnKF winds.

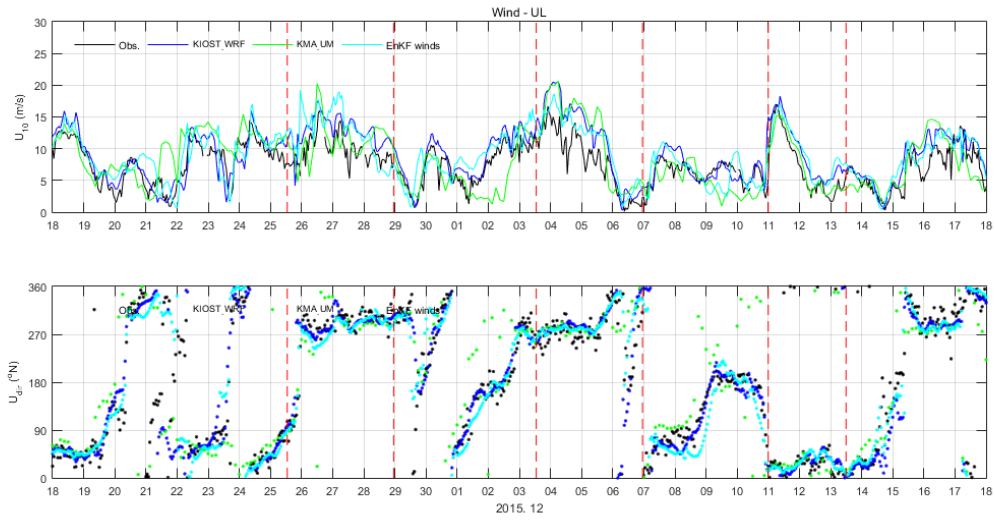


Figure 16 Time series of the UL wind observations and KIOST-WRF, KMA-UM and EnKF winds.

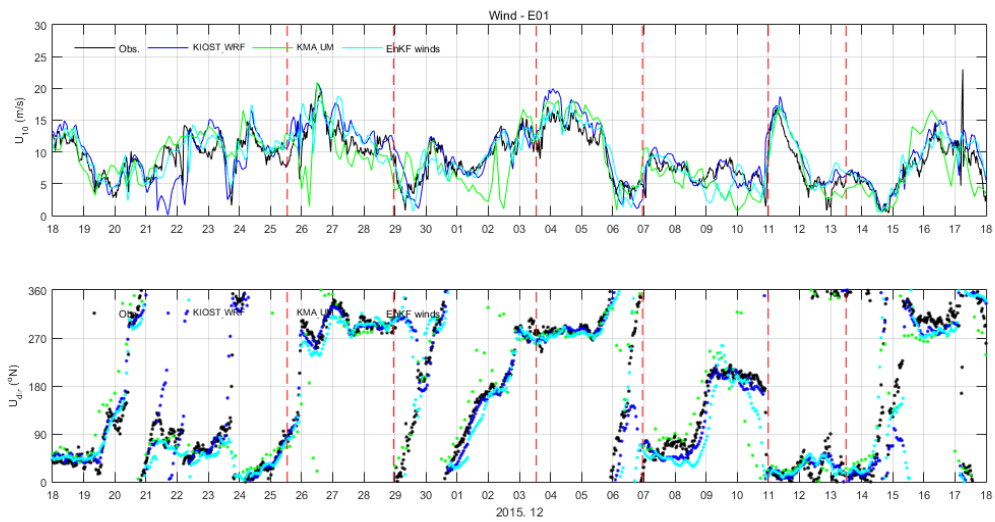


Figure 17 Time series of the E01 wind observations and KIOST-WRF, KMA-UM and EnKF winds.

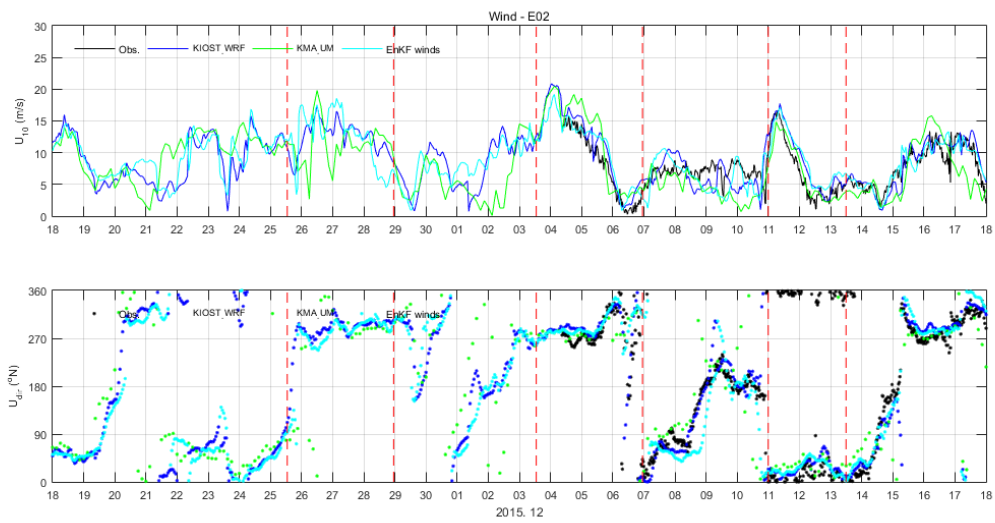


Figure 18 Time series of the E02 wind observations and KIOST-WRF, KMA-UM and EnKF winds.

During this period three storm periods (delineated with vertical dashed red lines in figures 9 to 18) have been examined in more detail:

- Storm 1 – from 25 November 13:00 until 28 November 23:00 KST - The period started with winds from Northeast over the whole East Sea of Korea followed by a strong cyclone with winds still from Northeast on the north-western side of the East Sea of Korea and rotating to North in the Tongjosen Man bay (offshore North Korea) and rotating further to Northwest in the southern part of the East Sea of Korea. The centre of the cyclone moves then further in the Northeast direction and the winds become predominantly from the Northwest along the coast of Korea and the southern part of the East Sea of Korea. Figure 19 shows a snapshot of the KIOST-WRF winds and Overall and Coastal model waves during this period. During this period the observed significant wave height is above 4 m nearshore and above 6 m offshore, the peak wave period is above 12 seconds and waves propagate from the Northeast nearshore and mostly Northwest offshore, although at UL and E01 waves are mostly towards the coast. Wind speeds peak at about 20 m/s at E01 offshore and blow from Northwest.

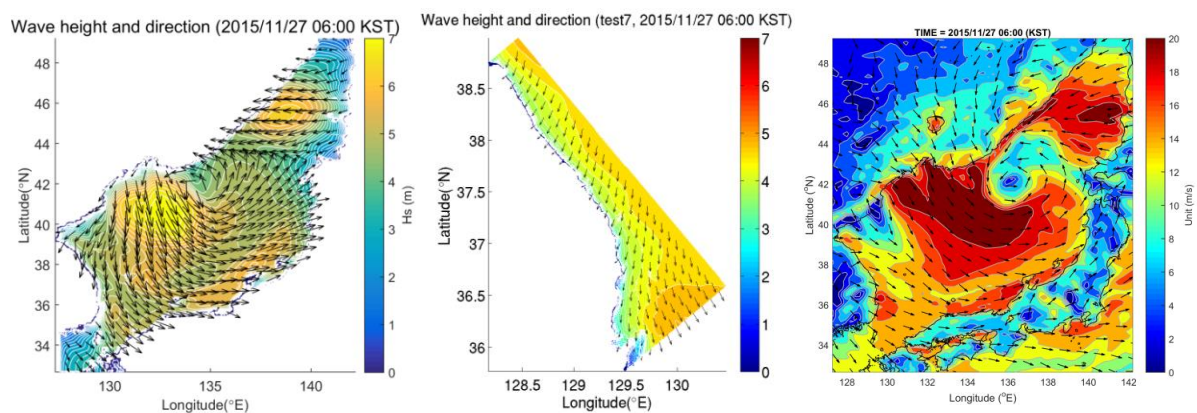


Figure 19 Snapshot of the Overall and Coastal model wave (left and middle panels) and KIOST-WRF wind fields (right panel) during Storm 1.

- Storm 2 – from 3 December 13:00 until 6 December 23:00 KST - The period started with winds from the West over the southern part of the East Sea of Korea which increased and got a more north-westerly direction, leading to high waves along the coast of Japan. Figure 20 shows a snapshot of the KIOST-WRF winds and Overall and Coastal model waves during this period. The wave conditions observed nearshore are very mild, with the significant wave height well below the 2 m and the peak wave period below 10 s, offshore the significant wave height can be as high as 5 m in E01. There are no wind observations at DH during this period and at E02 for the start of the period. At E01 and UL the observed winds are from the West-Northwest and at most 17 m/s.

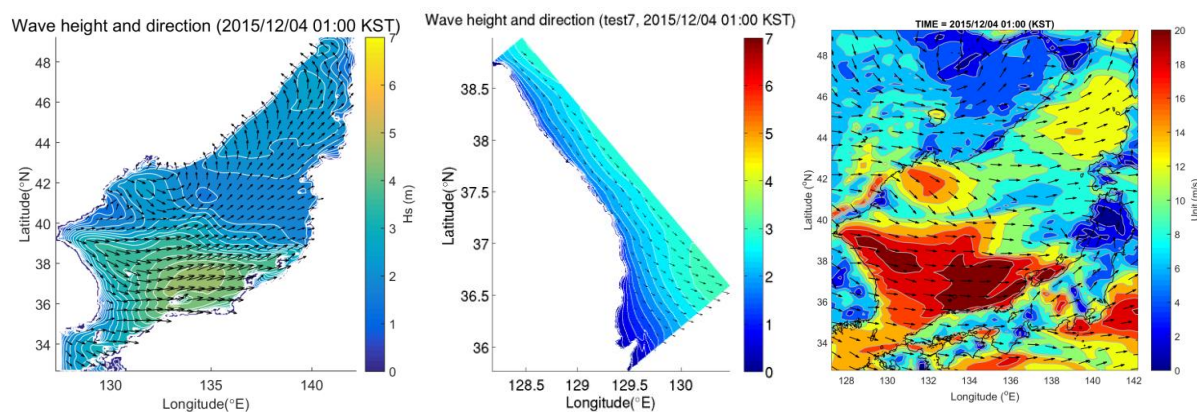


Figure 20 Snapshot of the wave (left and middle panels) and wind fields (right panel) during Storm 2.

- Storm 3 - from 11 December 00:00 until 15 December 12:00 KST - The period started with winds from Northeast over the whole East Sea of Korea which increased and got a more northern direction. Figure 21 shows a snapshot of the KIOST-WRF winds and Overall and Coastal model waves during this period. The observed waves are from the Northeast, the peak significant wave height is about 5m nearshore and above 6 m offshore; the peak wave period is about 10 seconds. Offshore the observed winds are also from the Northeast ranging between 15 and 20 m/s.

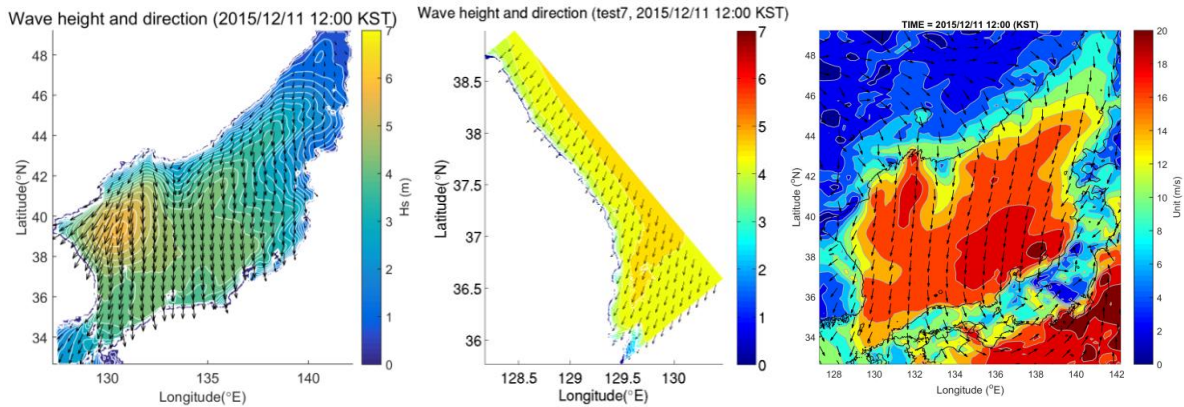


Figure 21 Snapshot of the wave (left and middle panels) and wind fields (right panel) during Storm 3.

The root-mean-square-errors of the wave and wind results for the whole period are given in Table 2 and Figure 22, respectively.

Location	U_{10}			U_{dir}		
	WRF	Enkf	UM	WRF	EnKF	UM
DH	2.6	3.2	2.5	60	62	76
UL	2.7	3.0	3.4	39	41	62
E01	2.5	2.1	3.0	38	38	56
E02	2.2	2.3	3.1	34	38	57

Table 2 Root-mean-square-errors (RMSE) of the atmospheric models KIOST-WRF and KMA-UM and determined by EnKF wind speeds and directions.

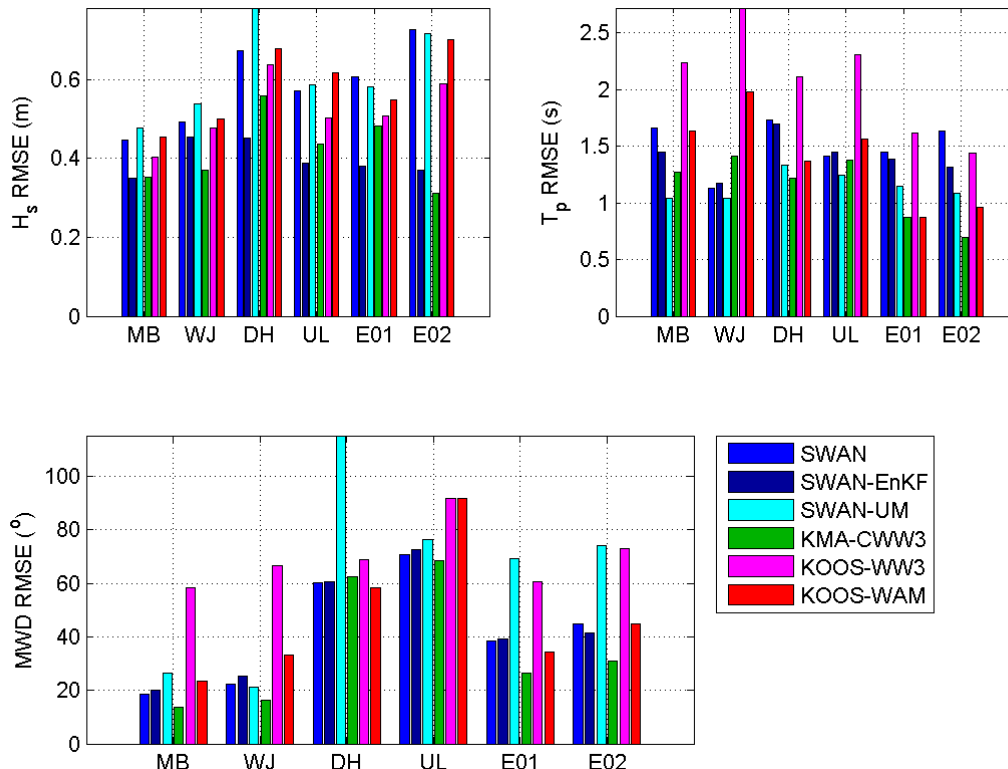


Figure 22 Root-mean-square-error (RMS) of the wave model results for 2015.

The following conclusions are taken from the analyses of the comparisons:

- At the coastal locations MB and WJ all models seem to follow the observation relatively well. All models overestimate the observed and relatively low significant wave height in Storm 2, except for the KMA-CWW3 model. Especially at MB, all models provide predictions very close to the observations during Storm 3. From the 17th of December the MWD data of KIOST-WW3 is faulty taking a fixed value of 180°N. No data from these locations have been assimilated but still the SWAN-EnKF results compare better with the H_s and T_p observations than those of SWAN. Especially during Storm 2 the SWAN-EnKF H_s and T_p data follow closer the observations.
- At nearshore DH location and offshore UL location the comparisons between the model significant wave height and peak wave period predictions and the observations are similar to those with the MB and WJ locations. Waves at these deep waters locations are not directly affected by the bathymetry and the performance of the models in terms of wave direction is comparable. The DH H_s observations have been assimilated and at this location and the H_s RMSE is much lower than that of the other models.
- At the further offshore E01 location all models seem to follow the significant wave height and mean wave direction observations relatively well. Again, except for the KMA-CWW3 model and the SWAN-EnKF results, all models underestimate the wave height in Storm 2, which at this location correspond to high significant wave heights, as high as those during Storm 3.
- There are no wave observations available from E02 during the period between the 15th of November and the 4th of December. During the period with observations the comparisons between the model predictions and the observations are similar to those at UL. Although the E02 data has not been assimilated the RMSE of the SWAN-EnKF results is about half of that of the SWAN results.
- The WRF, SWAN-EnKF and UM model predictions follow the observations reasonably well and show comparable error statistics with the RMSE of the WRF predictions being slightly lower. At location E02 there are no observations during the 1st storm. At the other locations the models tend to overestimate the wind speed, especially during the second half of the 1st storm. At location DH there are no observations during the 2nd storm and at all other locations the WRF and UM models overestimate the observed wind speeds. The EnKF data assimilation is successful in reducing the overestimation of the original WRF winds. Both the WRF and the UM predictions compare well with the observed wind speed peak during the 3rd storm period.

From these comparisons it can be concluded that the SWAN model already provided wave predictions with at least the same quality as that of the existing models for the region and that the errors in the wave predictions seem to be mostly due to errors in the wind predictions, with the EnKF data assimilation leading to results closer to the observations. In fact the EnKF lead for the whole period to reductions in the RMSE of H_s and T_p of up to 38% and 7%, respectively, in the locations where the data were assimilated. At the other locations the reductions were of up to 49% and 19% in the H_s and T_p ' RMSEs, respectively. The differences in the MWD' RMSE were not statistically significant. For the period of the second storm the reductions were larger and of up to 66% and 42% in the H_s and T_p ' RMSE in the locations where the data were assimilated and 75% and 36% in the H_s and T_p ' RMSE in the locations where the data were assimilated.

It is unclear whether the considered UM winds are indeed those that have been used to force the KMA-CWW3 model, given that the CWW3 results do not overestimate the wave conditions during the second storm period whereas the UM winds overestimate the observations and lead to wave height overestimates in the other models.

6 Final remarks

A SWAN wave model with EnKF data assimilation is being developed to respond to the need of wave forecasts for the East Coast of Korea. The validation of the model hindcasts during the considered storm period shows that the model results are at least as accurate as those of other available local model. The main contributor to the model errors appears to be the errors in the forcing wind fields. The EnKF assimilation of offshore significant wave height observations with the winds as control variable leads to reductions in the root-mean-square-error at locations other than those where the data were assimilated of about 50% and in the peak wave period of about 20%. The further development of the system will involve a sensitivity study to which other wave parameters should be assimilated and from which observation locations and assessment of the results in forecast mode.

Acknowledgment

We are thankful to ECMWF, KMA, KHOA and the KOOS project of KIOST for the having been able to access and use their data. We are, furthermore, grateful to the Korean Government for funding.

References

- Booij, N., Ris, R. C., and L. H. Holthuijsen, 1999: A third generation wave model for coastal regions. Part 1. Model description and validation, *J. Geophys. Res.*, 104(C4), 7649-7666.
- Dee, D. P. and co-authors, 2011: The ERA-Interim reanalysis: configuration and performance of the data assimilation system, *Q. J. R. Meteorol. Soc.*, 137 (656), 553-597, doi:10.1002/gj.828.
- Evensen, G., 2003: The ensemble Kalman filter: theoretical formulation and practical implementation. *Ocean Dynamics*. 53, 343-367.
- Hasselmann K., T.P. Barnett, E. Bouws, H. Carlson, D.E. Cartwright, K. Enke, J.A. Ewing, H. Gienapp, D.E. Hasselmann, P. Kruseman, A. Meerburg, P. Müller, D.J. Olbers, K. Richter, W. Sell, and H. Walden, 1973: *Measurements of wind-wave growth and swell decay during the Joint North Sea Wave Project (JONSWAP)*. *Ergänzungsheft zur Deutschen Hydrographischen Zeitschrift Reihe, A(8)*, Nr. 12, p.95.
- Heo, K.-Y. and T. Ha, 2016: Producing the Hindcast of Wind and Waves Using a High-Resolution Atmospheric Reanalysis around Korea. *Journal of Coastal Research: Special Issue 75 - Proceedings of the 14th International Coastal Symposium*, 1107 – 1111, Sydney 6-11 March 2016.
- Komen, G. J., L. Cavaleri, M. Donelan, K. Hasselmann, S. Hasselmann and P. A. E. M. Janssen, 1994: *Dynamics and Modelling of Ocean Waves*. Academic Press.
- Rogers, W.E., P.A. Hwang, and D.W. Wang. 2003: Investigation of wave growth and decay in the SWAN model: three regional-scale applications, *J. Phys. Oceanogr.*, 33, 366-389.
- Seo, S.-N., 2008: Digital 30sec Gridded Bathymetric Data of Korea Marginal Seas - KorBathy30s (in Korean), *Journal of Korean Society of Coastal and Ocean Engineer*, 20 (1), 110-120.
- Serpoushan, N., M. Zeinoddini and M. Golestani, 2013: An ensemble kalman filter data assimilation scheme for modeling the wave climate in Persian Gulf. *Proceedings of OMAE2013*, June 9-14, 2013, Nantes, France.
- Zijlema, M., G.Ph. van Vledder and L.H. Holthuijsen, 2012: Bottom friction and wind drag for wave models, *Coastal Engineering*, 65, 19-26.